International Journal of Antimicrobial Agents xxx (2011) xxx–xxx

Contents lists available at SciVerse ScienceDirect

International Journal of Antimicrobial Agents

journal homepage: http://www.elsevier.com/locate/ijantimicag

Effect of colistin exposure and growth phase on the surface properties of live *Acinetobacter baumannii* cells examined by atomic force microscopy

Rachel L. Soon[a], Roger L. Nation[a], Marina Harper[b,c], Ben Adler[b,c], John D. Boyce[b,c], Chun-Hong Tan[a], Jian Li[a,1], Ian Larson[a,*,1]

[a] *Facility for Anti-infective Drug Development and Innovation, Drug Delivery, Disposition and Dynamics, Monash Institute of Pharmaceutical Sciences, Monash University, 381 Royal Parade, Parkville, VIC 3052, Australia*
[b] *Department of Microbiology, Monash University, VIC, Australia*
[c] *Australian Research Council Centre of Excellence in Structural and Functional Microbial Genomics, Monash University, VIC, Australia*

ARTICLE INFO

Article history:
Received 7 March 2011
Accepted 26 July 2011

Keywords:
Atomic force microscopy
Colistin
Acinetobacter baumannii
Morphology
Surface properties

ABSTRACT

The diminishing antimicrobial development pipeline has forced the revival of colistin as a last line of defence against infections caused by multidrug-resistant Gram-negative 'superbugs' such as *Acinetobacter baumannii*. The complete loss of lipopolysaccharide (LPS) mediates colistin resistance in some *A. baumannii* strains. Atomic force microscopy was used to examine the surface properties of colistin-susceptible and -resistant *A. baumannii* strains at mid-logarithmic and stationary growth phases in liquid and in response to colistin treatment. The contribution of LPS to surface properties was investigated using *A. baumannii* strains constructed with and without the *lpxA* gene. Bacterial spring constant measurements revealed that colistin-susceptible cells were significantly stiffer than colistin-resistant cells at both growth phases ($P < 0.01$), whilst colistin treatment at high concentrations (32 mg/L) resulted in more rigid surfaces for both phenotypes. Multiple, large adhesive peaks frequently noted in force curves captured on colistin-susceptible cells were not evident for colistin-resistant cells. Adhesion events were markedly reduced following colistin exposure. The cell membranes of strains of both phenotypes remained intact following colistin treatment, although fine topographical details were illustrated. These studies, conducted for the first time on live *A. baumannii* cells in liquid, have contributed to our understanding of the action of colistin in this problematic pathogen.

1. Introduction

The 'post-antibiotic era' is approaching, with current antimicrobial development efforts proving insufficient to keep pace with the escalating rates of multidrug-resistant (MDR) pathogens [1]. Gram-negative pathogens such as *Acinetobacter baumannii* have recently taken the spotlight owing to an armamentarium of intrinsic and acquired resistance mechanisms [2]. Suggestions that the availability of an effective antibiotic against these 'superbugs' is still years away led to the revival of the 'old' polymyxins as a last line of defence, specifically colistin (polymyxin E) [3].

The ability of *A. baumannii* to remain viable for extensive periods within harsh environments facilitates nosocomial spread, thus presenting it as a major causative organism in a variety of hospital-acquired infections [4]. Worryingly, colistin heteroresistance has been detected in *A. baumannii* [5,6]; the presence of a resistant subpopulation within a susceptible strain [based on minimum inhibitory concentrations (MICs)] holds the potential to contribute to therapeutic failure [5]. This problematic situation has been compounded by recent evidence of extremely drug-resistant strains that are resistant to all current antibiotics, including colistin [7–9].

The exact mechanism of colistin's antibacterial activity remains unknown. However, the cationic amphipathic nature of colistin is considered essential to allow its self-promoted uptake across the Gram-negative outer membrane [10]. This complex, asymmetrical outer membrane structure comprises a tightly packed external lipopolysaccharide (LPS) leaflet and an internal phospholipid leaflet, together with proteins and lipoproteins [11]. LPS exhibits an amphipathic structure encompassing three domains; a highly conserved lipid A embedded within the membrane is attached to a core oligosaccharide, which is linked to a heterogeneous O-antigen side chain [12]. High-affinity electrostatic binding of colistin to anionic lipid A phosphoesters is proposed to result in the displacement of divalent cations that normally cross-bridge adjacent LPS molecules [10]. Subsequent destabilisation of the membrane facilitates insertion of the hydrophobic colistin domains, which disrupts the external leaflet enabling self-promoted uptake of colistin [10].

* Corresponding author. Tel.: +61 3 9903 9570; fax: +61 3 9903 9629.
E-mail address: ian.larson@monash.edu (I. Larson).
[1] These two senior authors contributed equally to this work.

0924-8579/$ – see front matter © 2011 Elsevier B.V. and the International Society of Chemotherapy. All rights reserved.
doi:10.1016/j.ijantimicag.2011.07.014

Polymyxin resistance in several bacterial species involves modifications to lipid A phosphate moieties, which decrease the negative surface charge and consequently diminish the electrostatic polymyxin–lipid A interaction [13–16]. For colistin-resistant *A. baumannii*, mutations have been detected in the same two-component system (PmrAB) [17,18] that regulates these lipid A substitutions [19]. Differences in protein expression have also been reported in comparison with colistin-susceptible strains [20]. Notably, a defective lipid A biosynthetic pathway has been identified in colistin-resistant *A. baumannii* strains arising from mutations within the *lpxA*, *lpxC* or *lpxD* genes encoding key enzymes involved in lipid A biosynthesis [21]. The resultant loss of LPS from colistin-resistant cells thus abates the crucial initial interaction necessary for colistin uptake.

The rapidly diminishing antimicrobial repertoire against *A. baumannii* demands that comprehension of the molecular basis for colistin action and resistance in *A. baumannii* be enhanced in order to prolong its lifespan and to provide a platform for the development of new agents. Atomic force microscopy (AFM) provides numerous benefits for such investigations [22]. Importantly, live bacteria can be observed in aqueous conditions mimicking the natural bacterial environment, without necessitating expensive and time-consuming sample manipulation procedures often required for other microscopic techniques [23]. In the present study, AFM was utilised to compare the surface properties of colistin-susceptible versus -resistant *A. baumannii* cells in liquid as well as their respective responses to colistin treatment. Previous reports that *A. baumannii* strains were less susceptible to colistin at stationary versus mid-logarithmic phase [24] provided the impetus to conduct these investigations as a function of growth phase.

2. Materials and methods

2.1. Chemicals

Colistin sulphate was obtained from Sigma-Aldrich (lot no. 109K1574; Sydney, NSW, Australia) and was dissolved in Milli-Q™ water (Millipore, Melbourne, VIC, Australia) to make a 1 mg/mL stock solution. Sterilisation was achieved by passage through 0.22 μm syringe filters (Sartorius, Melbourne, VIC, Australia), following which the solution was stored at 4 °C for up to 1 month, conditions under which colistin is stable [25].

2.2. Bacterial strains

Two colistin-heteroresistant *A. baumannii* strains (colistin MICs of 1 mg/L) were used: the *A. baumannii* type strain ATCC 19606 (American Type Culture Collection, Manassas, VA); and a clinical isolate FADDI-AB016. Colistin-resistant strains (MICs > 128 mg/L) were obtained from these parent strains and were termed 'R' strains. In addition, two complemented derivatives of strain 19606R were constructed [21] to examine the contribution of LPS to the cellular properties of *A. baumannii*: colistin-susceptible strain 19606R + *lpxA* (MIC = 1 mg/L) harboured the vector with the *lpxA* gene; whilst colistin-resistant 19606R + V (MIC > 128 mg/L) served as a control and contained the empty vector (V) only [21]. All strains were stored and prepared as previously described [26].

2.3. Bacterial sample preparation for atomic force microscopy analysis

Bacteria were immobilised on clean glass slides (Livingstone International Pty Ltd., Sydney, NSW, Australia) coated with gelatin using a procedure adapted from Doktycz et al. [27]. Briefly, gelatin solutions (0.5%) (Sigma-Aldrich) were prepared at ca. 60 °C and were filtered through 0.22 μm syringe filters under aseptic conditions. Glass slides were dipped into this solution and were left in a standing position to dry overnight. *Acinetobacter baumannii* cells were harvested from broth and were washed twice with Milli-Q water by centrifuging at 3000 × *g* for 5 min at 25 °C [28]. The resulting pellet was gently re-suspended in 300 μL of Milli-Q water and was deposited on gelatin-coated slides. Secure immobilisation of colistin-susceptible cells was attained after 30 min; however, colistin-resistant cells were left for up to 1 h. Slides were thoroughly rinsed with fresh Milli-Q water to remove any loosely bound cells.

The effect of colistin treatment on mid-logarithmic and stationary phase *A. baumannii* cells was examined by incubating bacteria with colistin at 1 mg/L and 32 mg/L for 20 min at 37 °C. Following centrifugation and washing, bacterial samples were prepared for AFM analysis as described above immediately prior to analysis. Colistin treatment of 19606R + *lpxA* and 19606R + V was not conducted at stationary phase.

2.4. Fluorescence labelling and confocal laser scanning microscopy (CLSM)

To determine the viability of untreated *A. baumannii* ATCC 19606 and 19606R, and of cells treated with 1 mg/L or 32 mg/L colistin for 20 min in broth culture and immobilised on gelatin-coated slides, a LIVE/DEAD BacLight™ Bacterial Viability Kit (L-7012; Molecular Probes®; Invitrogen, Newcastle, NSW, Australia) was employed. Slides were prepared and analysed in triplicate. The viability kit included the green fluorescent DNA-binding stain SYTO 9 (representing live bacteria) and the red fluorescent DNA-binding stain propidium iodide (representing a loss of viability). Equal proportions (1.5 μL) of both stains were mixed and diluted in Milli-Q water to 1 mL. Subsequently, 300 μL of this solution was added to each slide and was incubated in darkness for 30 min at room temperature. Slides were inverted and mounted on a microscope slide. Imaging was conducted with a Nikon TE2000U microscope (Nikon, Tokyo, Japan) coupled to a CoolSNAP fx low-light camera (Roper Scientific, Trenton, NJ) and illuminated using a Sutter Instruments DG-4 light box (Sutter Instrument Company, Novato, CA). Standard fluorescein and Texas red band pass filters were used to visualise SYTO 9 and propidium iodide, respectively. Images were processed using the software/hardware package MetaFluor (Universal Imaging, Downingtown, PA).

2.5. Imaging and force curve experiments

All imaging and force curve experiments were conducted in Milli-Q water using a Dimension™ 3000 atomic force microscope with a Digital Instruments NanoScope® IIIa controller (Veeco Instruments, Plainview, NY) operating in contact mode. V-shaped cantilevers (TR-400; Olympus Corp., CA) were employed with an average spring constant of 0.03 nN/nm, as determined using the thermal noise method [29]. The optical lever sensitivity (nm/V) of the cantilever was determined prior to each experiment from the slope of the contact region of a reference force curve obtained on a hard surface. Height and deflection images were obtained at a scan rate of 1 Hz. Six samples were prepared independently for each condition over two separate days, and multiple large scans (20 μm × 20 μm) were performed on separate sections of the slides to validate the reproducibility of the observations. High magnification images (5 μm × 5 μm) were subsequently captured at 512 pixels per line to present greater surface detail and to facilitate quantitative measurements of bacterial dimensions.

For force experiments, measurements between colistin-susceptible and -resistant subpopulations of the same strain were performed using the same cantilever. However, for each separate paired strain a new cantilever was utilised to minimise the risk

Please cite this article in press as: Soon RL, et al. Effect of colistin exposure and growth phase on the surface properties of live *Acinetobacter baumannii* cells examined by atomic force microscopy. Int J Antimicrob Agents (2011), doi:10.1016/j.ijantimicag.2011.07.014

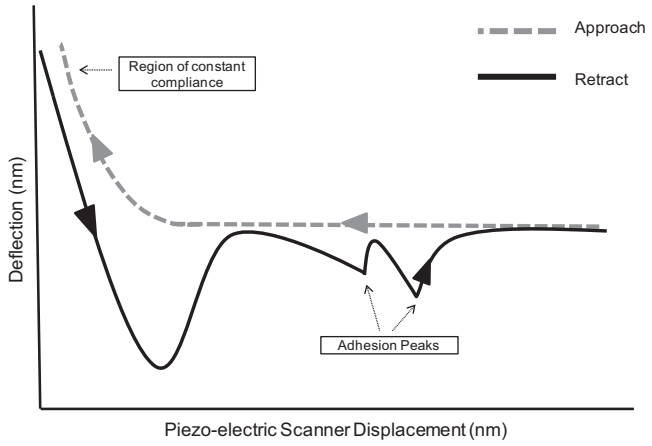

Fig. 1. Representative atomic force microscopy (AFM) force curves illustrating the approach and retraction of an AFM tip on a bacterial cell.

of contamination. The values reported thus enable relative comparisons to be performed between phenotypes. The AFM tip was made to approach a bacterium at a speed of 0.5 Hz, with a ramp size of 2 μm, and to indent the surface until a trigger threshold was reached. Subsequently, the tip was retracted from the surface at the same speed. A force curve was constructed from each approach–retract cycle (Fig. 1). Care was taken to avoid peripheral areas as changes in contact area between the tip and sample have been demonstrated to influence force measurements [30]. For each sample, at least 20 force curves were acquired on a minimum of 10 cells, at four different positions on the cell surface.

2.6. Force curve analysis

Analysis of force curves was performed using the Scanning Probe Image Processing software (SPIP™; Image Metrology, Hørsholm, Denmark). The cantilever sensitivity was used together with the cantilever spring constant (k_c) to convert raw AFM data into deflection (nm) versus piezo displacement (nm) curves (Fig. 1) [31,32]. The slope (s) of the 'region of constant compliance' (Fig. 1) was applied to the following equation to calculate the bacterial spring constant (k_b) as a measure of cellular stiffness [33]:

$$k_b = \frac{k_c s}{1 - s}$$

A total of 10 curves were analysed per cell and the mean and standard deviation (S.D.) of the sample were calculated based on the k_b of 10 cells (i.e. a total of 100 force curves per test condition). Analysis of variance (ANOVA) and two-sample t-tests were employed for statistical analyses (GraphPad Prism v5.0; GraphPad Software Inc., La Jolla, CA).

An adhesion event was defined as a sharp peak in the retraction profile (Fig. 1) [34]. For each adhesion peak (from 100 force curves), the adhesion force and distance between the cantilever and cell were recorded [34]. Histograms describing the distribution of forces and distances were constructed for each strain at both growth phases. The number of adhesion peaks (n) as well as the mean, S.D., median and range of distances and forces were tabulated for each sample at both growth phases.

3. Results

3.1. Cell viability

CLSM images were acquired to assess the viability of colistin-susceptible *A. baumannii* ATCC 19606 and colistin-resistant 19606R cells (data not shown). Colistin-resistant cells required 1 h to adhere securely to the gelatin surface; colistin-susceptible cells were immobilised after only 15 min. For both strains, untreated cells and cells treated with 1 mg/L colistin stained green, indicating that viability was retained following immobilisation. Following treatment with 32 mg/L colistin, both *A. baumannii* ATCC 19606 and 19606R cells aggregated into large clusters; the majority of colistin-susceptible cells appeared non-viable, whereas colistin-resistant cells were mainly viable.

3.2. Mechanical properties of colistin-susceptible and -resistant *Acinetobacter baumannii*

Comparison of the bacterial spring constant (k_b) between mid-logarithmic and stationary growth phases did not yield a difference (ANOVA; $P > 0.05$) for colistin-susceptible and -resistant strains (Fig. 2A). In contrast, colistin-susceptible cells yielded a higher mean k_b than that of their paired colistin-resistant cells at each respective growth phase (ANOVA; $P < 0.01$). However, this difference was not significant for colistin-susceptible 19606R + *lpxA* versus colistin-resistant 19606R + V strains (Fig. 2A) (t-test post-hoc analysis, $P > 0.05$), which were complemented with an *lpxA* gene and empty vector, respectively [21]. The k_b of 19606R + *lpxA* was significantly lower than that of ATCC 19606 at both growth phases (Fig. 2A) (t-test, $P < 0.05$). No differences were observed between the k_b of colistin-resistant strains 19606R + V and 19606R (Fig. 2A) (t-test, $P > 0.05$).

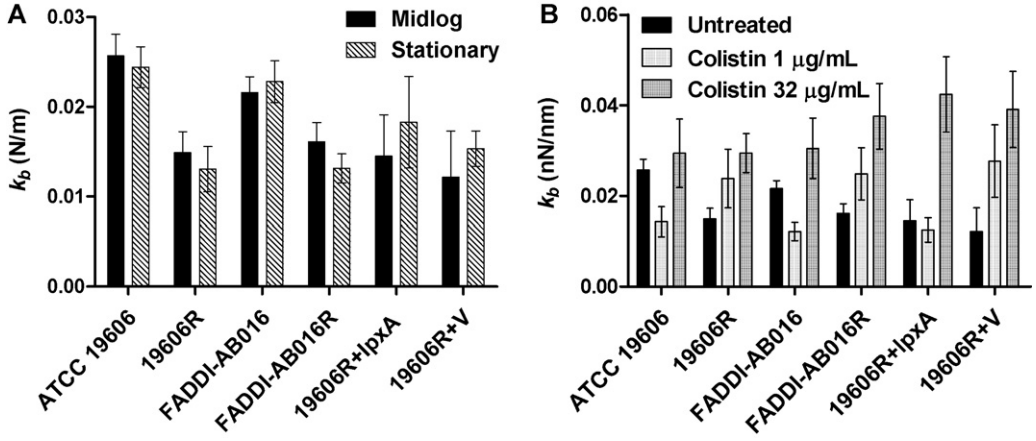

Fig. 2. (A) Bacterial spring constant (k_b) of untreated colistin-susceptible and -resistant *Acinetobacter baumannii* at mid-logarithmic and stationary growth phases. (B) Change in k_b following treatment of mid-logarithmic cells with 1 mg/L or 32 mg/L colistin.

Please cite this article in press as: Soon RL, et al. Effect of colistin exposure and growth phase on the surface properties of live *Acinetobacter baumannii* cells examined by atomic force microscopy. Int J Antimicrob Agents (2011), doi:10.1016/j.ijantimicag.2011.07.014

Table 1
Total number of adhesion events (*n*) as well as the mean, standard deviation (S.D.), median and range of distances and forces recorded for the adhesion peaks noted for each strain. Data were acquired from analysis of 100 force curves captured on colistin-susceptible and -resistant *Acinetobacter baumannii* strains at mid-logarithmic and stationary phases.

Growth phase/*A. baumannii* strain	*n*	Distance (μm)				Force (nN)			
		Mean	S.D.	Median	Range	Mean	S.D.	Median	Range
Mid-logarithmic phase									
ATCC 19606	159	0.641	0.201	0.629	1.08	6.94	3.13	5.98	14.0
19606R	69	0.658	0.178	0.625	0.823	4.02	1.50	3.80	7.17
FADDI-AB016	118	0.665	0.218	0.630	0.874	5.85	2.64	5.29	13.3
FADDI-AB016R	83	0.552	0.163	0.532	0.629	4.05	1.19	3.96	6.65
19606R + *lpxA*	208	0.778	0.241	0.752	1.21	9.08	4.17	8.42	17.8
19606R + V	77	0.722	0.253	0.670	1.08	6.35	2.45	6.11	10.22
Stationary phase									
ATCC 19606	212	0.637	0.172	0.615	0.870	6.14	3.18	5.51	14.8
19606R	118	0.674	0.177	0.629	0.774	5.61	1.78	5.46	8.59
FADDI-AB016	165	0.708	0.269	0.726	1.38	6.42	2.48	6.02	17.8
FADDI-AB016R	99	0.580	0.197	0.574	0.871	4.78	1.65	4.74	6.75
19606R + *lpxA*	175	0.796	0.202	0.760	0.948	6.99	2.17	6.61	11.5
19606R + V	89	0.674	0.184	0.661	0.732	5.96	2.41	5.49	12.9

Colistin treatment with 1 mg/L caused a reduction in the k_b of colistin-susceptible cells at mid-logarithmic phase in comparison with untreated cells (Fig. 2B) (ANOVA, $P < 0.05$); this value was noted to increase following exposure to 32 mg/L colistin (Fig. 2B) (ANOVA, $P < 0.05$). Conversely, colistin treatment with both concentrations elevated the k_b of colistin-resistant cells at mid-logarithmic phase (Fig. 2B) (ANOVA, $P < 0.05$). An identical trend was detected for paired strains ATCC 19606 and FADDI-AB016 at stationary phase in response to colistin exposure (data not shown).

3.3. Adhesion characteristics of colistin-susceptible and -resistant *Acinetobacter baumannii*

With the exception of the complemented strain (19606R + *lpxA*), the total number of adhesion events recorded for all strains at mid-logarithmic phase was considerably less than at stationary phase (Table 1). Multiple, large adhesive peaks were frequently observed in AFM force curves captured for untreated colistin-susceptible cells at both mid-logarithmic and stationary phase (Fig. 3A and D, respectively). In contrast, smooth retraction curves were

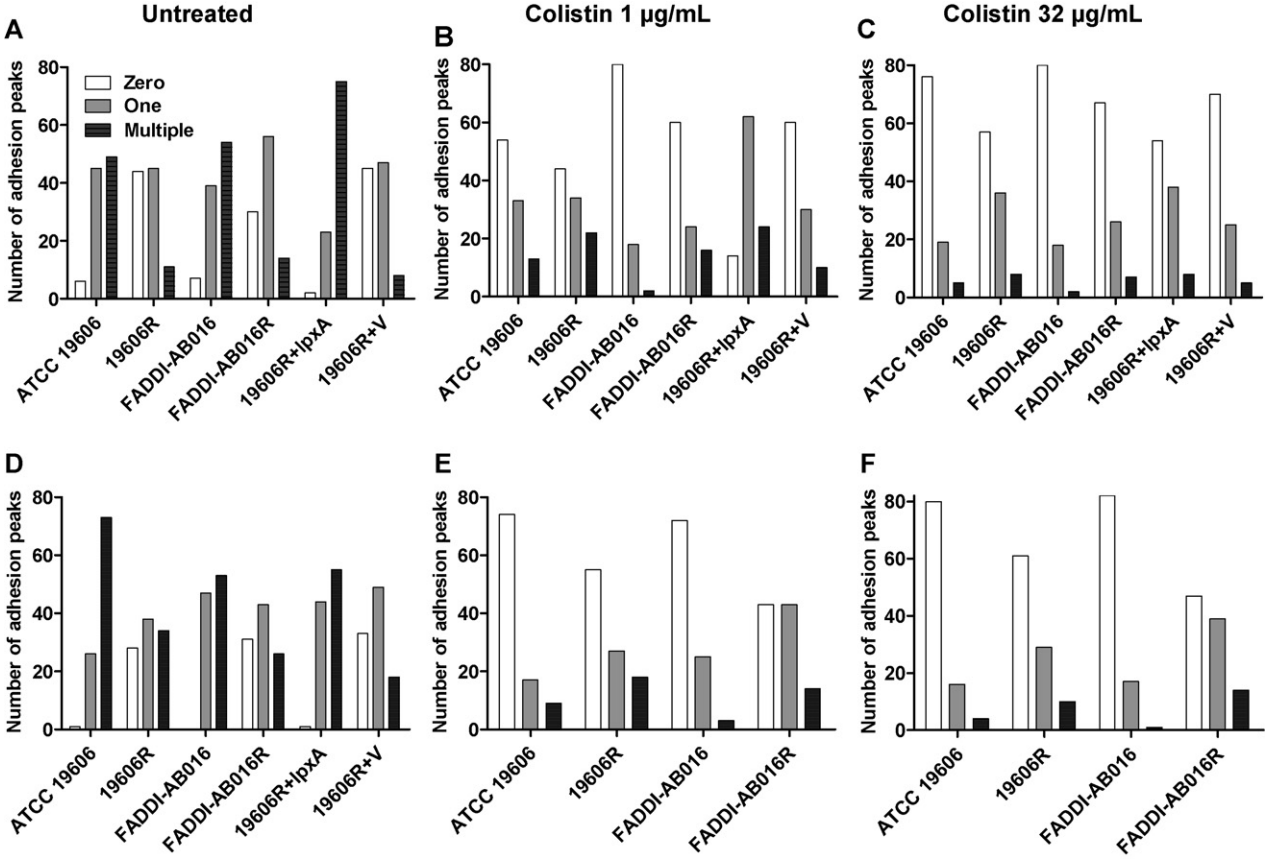

Fig. 3. Atomic force microscopy force curves captured on (A–C) mid-logarithmic phase and (D–F) stationary phase *Acinetobacter baumannii* strains with zero, one or multiple adhesion events per curve, for untreated cells (A and D) and for cells treated for 20 min with 1 mg/L colistin (B and E) or 32 mg/L colistin (C and F). Complemented strains (19606R + *lpxA* and 19606R + V) were not treated at stationary phase. For each strain at each condition, 100 force curves were analysed.

Please cite this article in press as: Soon RL, et al. Effect of colistin exposure and growth phase on the surface properties of live *Acinetobacter baumannii* cells examined by atomic force microscopy. Int J Antimicrob Agents (2011), doi:10.1016/j.ijantimicag.2011.07.014

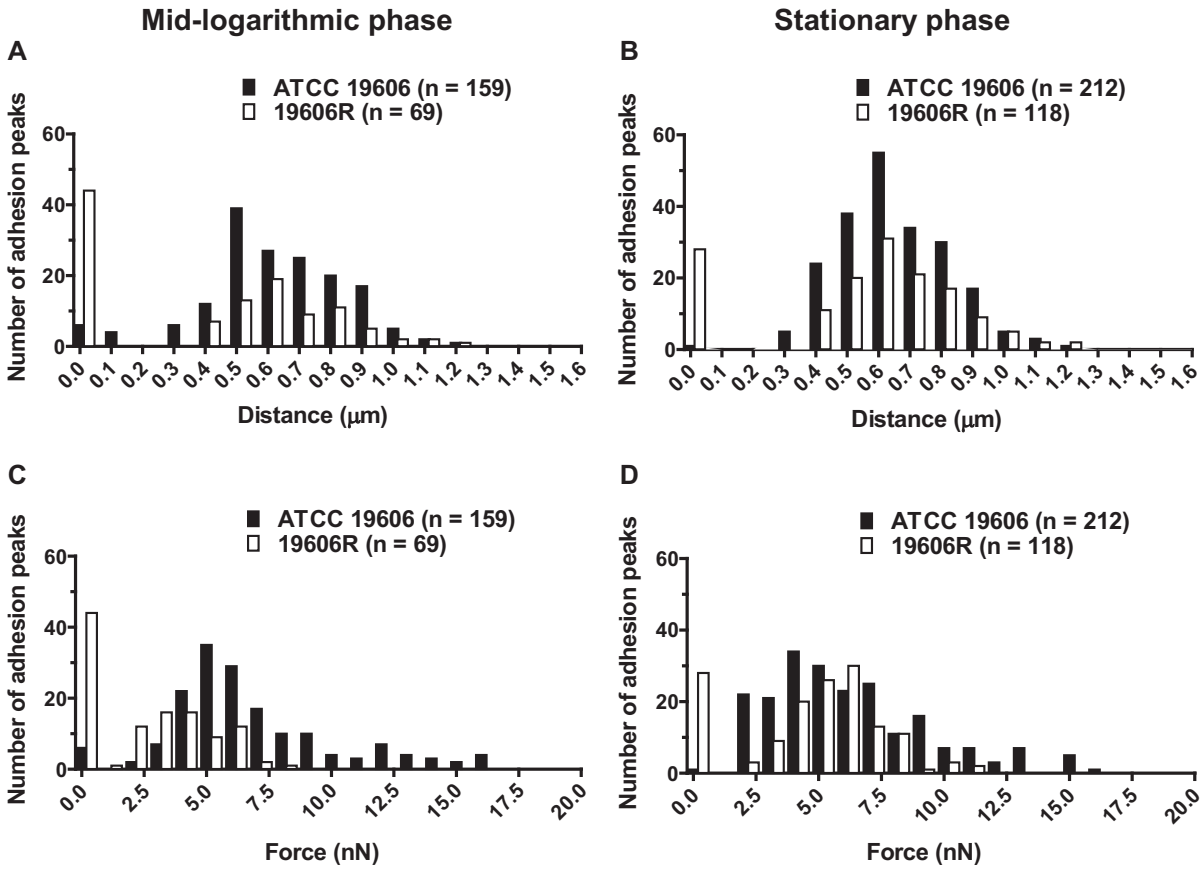

Fig. 4. Distribution of (A and B) adhesion distances and (C and D) forces upon retraction of the atomic force microscopy tip from the cell surface for colistin-susceptible *Acinetobacter baumannii* ATCC 19606 versus colistin-resistant 19606R at mid-logarithmic phase (A and C) and stationary phase (B and D).

commonly illustrated for colistin-resistant cells at both growth phases, with a large proportion of curves (ca. 30–45%) exhibiting no adhesion events (Fig. 3A and D).

Bacterial adhesion events are notoriously characterised by a high degree of variability [34], likely attributed to the heterogeneous nature of the outer membrane. Variability was reflected by large S.D. from the mean force and distance values; consequently, the median and range values are presented in Table 1. In addition, histograms illustrating the frequency distribution of forces and distances for *A. baumannii* ATCC 19606 and 19606R at mid-logarithmic and stationary phases are displayed in Fig. 4. Histograms displaying similar trends were constructed for paired strain FADDI-AB016 and 19606R complemented strains (data not shown). For all strains, adhesion distances and forces distributed over a larger range for colistin-susceptible versus -resistant cells at both growth phases (Table 1). The median adhesion distances for colistin-susceptible strains (FADDI-AB016 and 19606R + *lpxA*) were greater than those observed for their paired colistin-resistant strains (FADDI-AB016R and 19606R + V, respectively) (Table 1). However, comparison of ATCC 19606 versus 19606R revealed similar median pull-off distances at mid-logarithmic and stationary growth phases (Table 1). The median force of adhesion for all colistin-susceptible strains was larger than that for colistin-resistant strains at both growth phases. Adhesion events were markedly reduced following colistin treatment with 1 mg/L (Fig. 3B and E) and 32 mg/L (Fig. 3C and F) for both phenotypes, with a substantial increase in the number of curves exhibiting no adhesion.

3.4. Morphology of colistin-susceptible and -resistant *Acinetobacter baumannii*

Typical AFM images in Milli-Q water of *A. baumannii* ATCC 19606 and 19606R at mid-logarithmic phase are presented in Fig. 5A and D, respectively. Rod-like colistin-susceptible cells (mean length ± S.D. 2.62 ± 0.40 μm; $n = 15$) were clearly differentiated (*t*-test, $P < 0.001$) from the mostly spherical colistin-resistant cells (1.72 ± 0.25 μm; $n = 15$). Resistant cells primarily formed small clusters, chains or pairs. An extremely smooth surface topography was observed for both strains and extracellular appendages were not visible. Colistin-susceptible cells became elongated at stationary phase, with some cells extending up to ca. 12 μm (Fig. 6A). Elongation of colistin-resistant cells into short rod-like forms and extended structures (up to 7 μm) was also apparent (data not shown). Dimensions of the colistin-susceptible complemented strain 19606R + *lpxA* (2.58 ± 0.29 μm; $n = 15$) were indistinguishable from ATCC 19606. Similarly, the diameter of colistin-resistant 19606R + V was not different from 19606R (*t*-test, $P > 0.05$). FADDI-AB016 (2.15 ± 0.34 μm; $n = 15$) and FADDI-AB016R (1.65 ± 0.27 μm; $n = 15$) were smaller than their respective ATCC 19606 counterparts (*t*-test, $P < 0.05$).

Bacterial cells appeared intact and dimensions were maintained following colistin treatment of mid-logarithmic phase colistin-susceptible ATCC 19606 and colistin-resistant 19606R at 1 mg/L (Fig. 5B and E) and 32 mg/L (Fig. 5C and F). Interestingly, finer details of surface topography were evident

Please cite this article in press as: Soon RL, et al. Effect of colistin exposure and growth phase on the surface properties of live *Acinetobacter baumannii* cells examined by atomic force microscopy. Int J Antimicrob Agents (2011), doi:10.1016/j.ijantimicag.2011.07.014

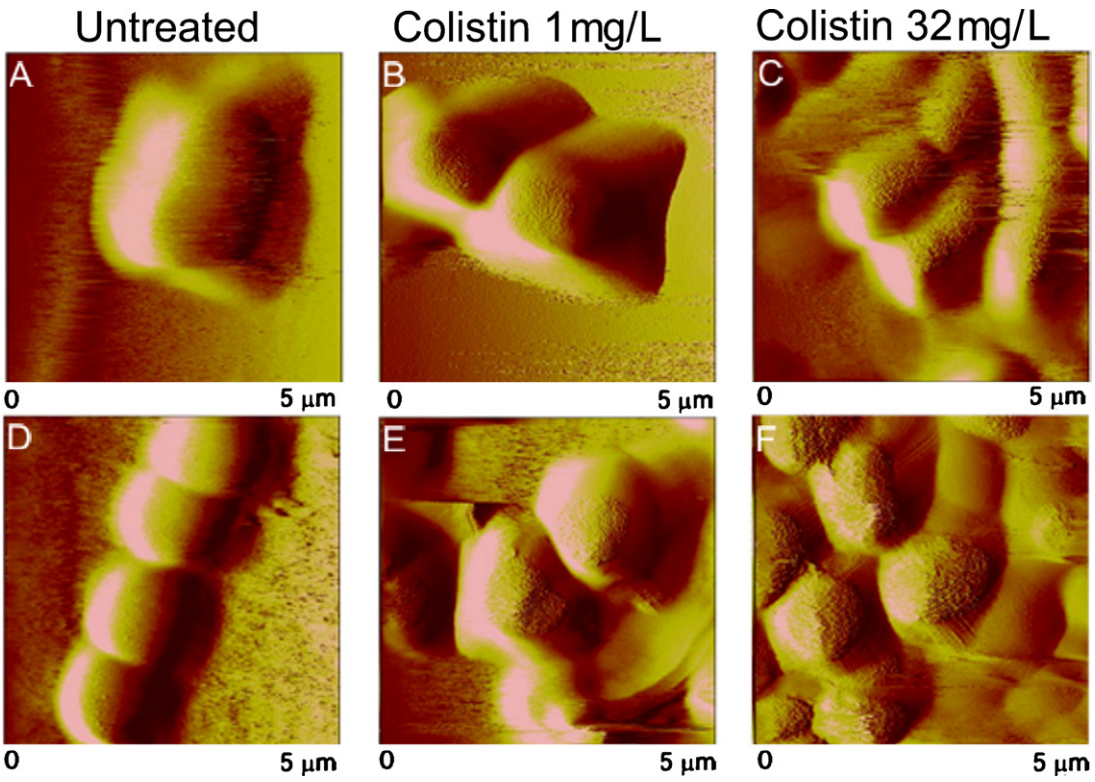

Fig. 5. Atomic force microscopy images (5 μm × 5 μm) of mid-logarithmic (A–C) colistin-susceptible *Acinetobacter baumannii* ATCC 19606 and (D–F) colistin-resistant 19606R illustrating untreated cells (A and D) and cells treated for 20 min with 1 mg/L colistin (B and E) or 32 mg/L colistin (C and F).

from images of colistin-treated cells. Considerable aggregation of both strains illustrated after exposure to colistin 32 mg/L (Fig. 5C and F) was consistent with confocal micrographs (data not shown). Similar results were obtained for all other strains at mid-logarithmic phase. Comparable images of colistin-treated paired ATCC 19606 (Fig. 6) and FADDI-AB016 (data not shown) strains at stationary phase were also obtained.

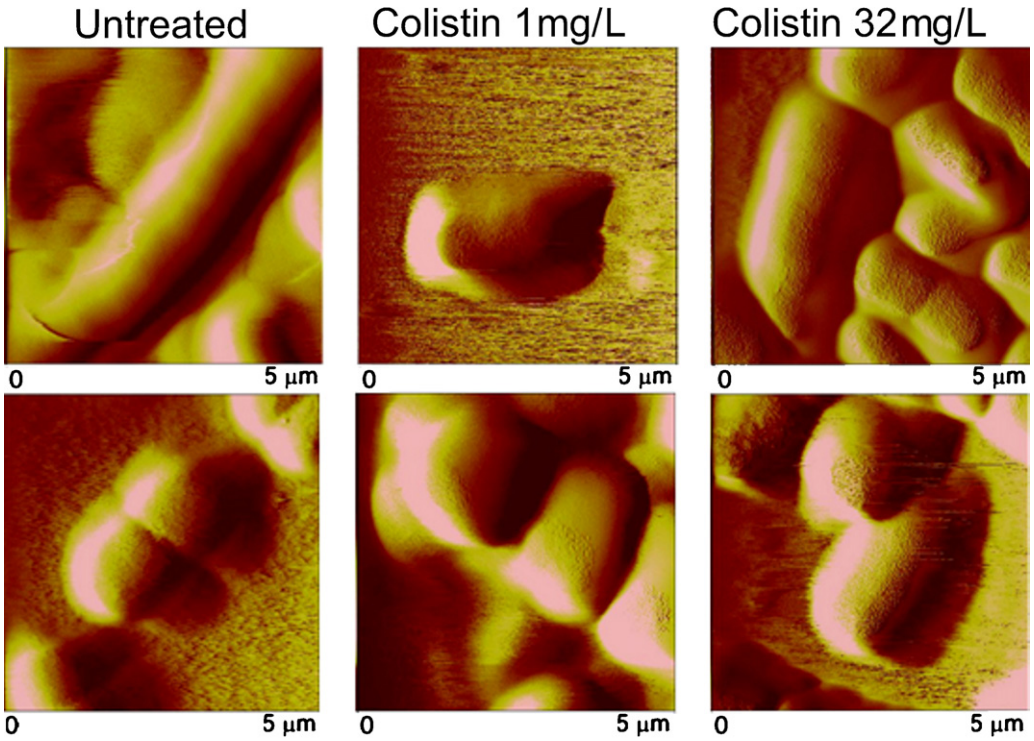

Fig. 6. Atomic force microscopy images (5 μm × 5 μm) of stationary-phase (A–C) colistin-susceptible *Acinetobacter baumannii* ATCC 19606 and (D–F) colistin-resistant 19606 illustrating untreated cells (A–D) and cells treated for 20 min with 1 mg/L colistin (B and E) or 32 mg/L colistin (C and F).

Please cite this article in press as: Soon RL, et al. Effect of colistin exposure and growth phase on the surface properties of live *Acinetobacter baumannii* cells examined by atomic force microscopy. Int J Antimicrob Agents (2011), doi:10.1016/j.ijantimicag.2011.07.014

4. Discussion

The need for a greater understanding of colistin activity and resistance has been reinforced by the rising incidence of colistin-heteroresistant MDR *A. baumannii* strains [9]. Since the advent of AFM, the capacity of this technique to investigate outer membrane alterations following antibiotic treatment has been demonstrated [35]. The basic principle underlying AFM relies on the sensing of forces between a sharp tip and the bacterial surface. Forces are detected with piconewton sensitivity upon approach and retraction of the tip to the bacterial surface, thus facilitating investigations of mechanical stiffness and adhesion characteristics [35,36]. In addition, as the tip scans across the sample, topographical images are obtained with nanometre-scale resolution.

Morphological differentiation between colistin-susceptible and -resistant *A. baumannii* has been documented from AFM images captured on dried cells in air [28]. The present study examined for the first time *A. baumannii* cells in an aqueous environment where the force exerted by the AFM tip on bacteria is reduced by a factor of 10–100 [37]; cell deformation is thus minimised and forces are measured with greater accuracy. AFM sample preparation procedures need to ensure that immobilisation is secure enough to prevent cells being swept away by the scanning tip, whilst preserving bacterial integrity and viability. Here we have adopted a procedure from Doktycz et al. [27] to immobilise *A. baumannii* on a layer of gelatin, providing a means of physical attachment whilst leaving the exposed cellular surface in its native state. The role of fimbriae [38] and LPS [39] in bacterial adhesion has been documented. With this in mind, the LPS-deficient outer membrane of colistin-resistant *A. baumannii* [21] may account for its lower tendency to attach to gelatin-coated slides in comparison with its colistin-susceptible counterpart. Confocal micrographs confirmed the viability of untreated immobilised colistin-susceptible and-resistant *A. baumannii* cells. Live cells were apparent following exposure to colistin at both MIC (1 mg/L) and supra-MIC (32 mg/L) concentrations, supporting our understanding that these likely represent the most resistant subpopulation.

To compare the mechanical properties of colistin-susceptible and -resistant *A. baumannii*, the bacterial spring constant (k_b) was ascertained, which describes changes to two factors, namely bacterial turgor pressure and rigidity [40]. The stiff gel-like structure of the outer membrane has been attributed to divalent cations bridging neighbouring LPS molecules, together with lateral interactions between saturated hydrocarbon lipid A chains [41]. Accordingly, the LPS deficiency of colistin-resistant *A. baumannii* cells [21] provides a plausible explanation for the lower k_b detected in this population, implying a softer leaflet of greater permeability compared with susceptible cells. Colistin-resistant *A. baumannii* strains have indeed been shown to be more permeable to a range of lipophilic antibiotics [42] as well as a hydrophobic fluorescent probe (1-*N*-phenylnaphthylamine [21]) used as a marker of membrane integrity. Although complementation with *lpxA* restored LPS production in strain 19606R + *lpxA* [21], the observation that these cells were softer than ATCC 19606 (Fig. 2A) (*t*-test, $P < 0.05$) may suggest that 19606R + *lpxA* expresses a reduced surface LPS content.

Interestingly, a reduction in k_b has been documented following exposure of Gram-negative bacterial strains to antimicrobial agents [43–45]. Similarly, colistin-induced destabilisation of the LPS monolayer of colistin-susceptible *A. baumannii* upon treatment with MIC concentrations (1 mg/L) may account for the decreased k_b observed (Fig. 2B). In contrast, stiffening of colistin-susceptible *A. baumannii* following 32 mg/L treatment (Fig. 2B) may be attributed to the saturation of specific LPS binding sites by colistin, which potentially amplifies the degree of non-specific binding to colistin-susceptible cells [26]. Accumulation of colistin at the outer membrane may thus increase the rigidity of the cellular architecture through various mechanisms, which deserve further examination. Indeed, the notion that colistin associates with the peptidoglycan layer of *P. aeruginosa* has been advanced [46]. Reports also support the ability of cationic antibiotics to alter the packing of LPS molecules, resulting in LPS aggregates of increased rigidity [47,48]. For LPS-deficient colistin-resistant *A. baumannii*, colistin must bind and incorporate into the outer membrane entirely in a non-specific fashion, thus accounting for the increased k_b observed after colistin exposure (Fig. 2B).

Multiple binding events ascribed to the extension of surface polymers have been documented in AFM bacteriological investigations [34]. Analogously, the 'saw tooth' appearance (Fig. 1) of our retraction force profiles of untreated colistin-susceptible *A. baumannii* at both growth phases reflects a non-specific binding pattern [34]. The retraction force profiles also provide information about the strength of adhesion events as well as the length of extracellular appendages as they attach to the tip and stretch upon retraction before the final unbinding event. Attempts to correlate AFM adhesion measurements with LPS length have failed to reveal a clear relationship for *Escherichia coli* [49,50]. However, development of outer membrane constituents throughout bacterial growth can account for the increased number of adhesion events noted for *A. baumannii* cells at stationary versus mid-logarithmic phase (Table 1; Fig. 3). Structural outer membrane differences can similarly account for the reduction in the number and force of adhesion events recorded for colistin-resistant versus -susceptible *A. baumannii* at both growth phases (Fig. 4). In support of this, short appendages sparsely distributed around the periphery of colistin-resistant *A. baumannii* have been illustrated previously [28]; these observations reflect a loss of LPS [21] as well as an altered expression of outer membrane proteins and fimbriae [20]. For colistin-susceptible *A. baumannii*, the lack of adhesion following colistin treatment may be attributed to the colistin–LPS interaction resulting in alterations to the tip–bacterium adhesion force. Non-specific interactions between colistin and other membrane constituents may explain the reduced adhesion noted for colistin-resistant *A. baumannii*. Further investigation is warranted as the complex chemistry of the typical AFM probes employed precludes further analysis of specific tip–bacterium interactions.

Both colistin-susceptible (Fig. 5A) and -resistant (Fig. 5D) cells appeared smooth and featureless, consistent with the understanding that the level of AFM image resolution achieved under liquid is considerably less than in air. This may be explained by the dynamic properties of cellular appendages [51]; thus, these AFM images reflect the average configuration of flexible appendages that are in a continuous state of disorder in a liquid environment. The rod-like versus spherical morphology of colistin-susceptible versus -resistant *A. baumannii*, respectively [28], was verified in the present investigation on live hydrated cells (Figs. 5 and 6). Morphological characteristics of the complemented strains (19606R + *lpxA* and 19606R + V) were equivalent to ATCC 19606 and 19606R, respectively, suggesting that differences between colistin-susceptible and -resistant *A. baumannii* are related to the *lpxA* mutation and LPS deficiency. A greater tendency for colistin-resistant cells to aggregate may arise from alterations to surface charge [26] and hydrophobicity resulting from the lack of LPS [21]. Indeed, increased cohesion has been described for *P. aeruginosa* mutants possessing truncated LPS structures [39,52]. Following colistin treatment, topographical details of both phenotypes were revealed (Figs. 5 and 6), attributed to the effect of colistin on appendages that minimises steric interference with the AFM tip. Additional support contributed by surrounding cells within the bacterial network may offer an alternative explanation for the elevated k_b detected both for colistin-susceptible and -resistant cells within the cluster following colistin 32 mg/L treatment (Fig. 2).

Please cite this article in press as: Soon RL, et al. Effect of colistin exposure and growth phase on the surface properties of live *Acinetobacter baumannii* cells examined by atomic force microscopy. Int J Antimicrob Agents (2011), doi:10.1016/j.ijantimicag.2011.07.014

In conclusion, this study is the first to employ AFM to examine the surface properties and morphology of colistin-susceptible and -resistant *A. baumannii* cells in liquid, including LPS-deficient mutant strains. The softer surface and reduced adhesion of spherical colistin-resistant versus rod-shaped colistin-susceptible cells corresponds with the loss of LPS reported for the resistant phenotype. Reduced adhesion and increased cellular rigidity following colistin treatment of colistin-susceptible and -resistant cells reflects specific interactions between colistin and LPS as well as non-specific interactions with outer membrane constituents, respectively. This study has provided important insight into our understanding of the action of colistin in this problematic pathogen.

Funding: This study was supported by a project grant awarded to RLN, JDB and JL by the Australian National Health and Medical Research Council (NHMRC). RLN and JL are supported by research grants from the National Institute of Allergy and Infectious Diseases of the National Institutes of Health (R01A107896 and R01A1079330). JL is an Australian NHMRC Senior Research Fellow.

Competing interests: None declared.

Ethical approval: Not required.

References

[1] Boucher HW, Talbot GH, Bradley JS, Edwards JE, Gilbert D, Rice LB, et al. Bad bugs, no drugs: no ESKAPE! An update from the Infectious Diseases Society of America. Clin Infect Dis 2009;48:1–12.
[2] Giamarellou H, Poulakou G. Multidrug-resistant Gram-negative infections: what are the treatment options? Drugs 2009;69:1879–901.
[3] Nation RL, Li J. Colistin in the 21st century. Curr Opin Infect Dis 2009;22:535–43.
[4] Munoz-Price LS, Weinstein RA. *Acinetobacter* infection. N Engl J Med 2008;358:1271–81.
[5] Hernan RC, Karina B, Gabriela G, Marcela N, Carlos V, Angela F. Selection of colistin-resistant *Acinetobacter baumannii* isolates in postneurosurgical meningitis in an intensive care unit with high presence of heteroresistance to colistin. Diagn Microbiol Infect Dis 2009;65:188–91.
[6] Li J, Rayner CR, Nation RL, Owen RJ, Spelman D, Tan KE, et al. Heteroresistance to colistin in multidrug-resistant *Acinetobacter baumannii*. Antimicrob Agents Chemother 2006;50:2946–50.
[7] Park YK, Peck KR, Cheong HS, Chung DR, Song JH, Ko KS. Extreme drug resistance in *Acinetobacter baumannii* infections in intensive care units, South Korea. Emerg Infect Dis 2009;15:1325–7.
[8] Doi Y, Husain S, Potoski BA, McCurry KR, Paterson DL. Extensively drug-resistant *Acinetobacter baumannii*. Emerg Infect Dis 2009;15:980–2.
[9] Peleg AY, Seifert H, Paterson DL. *Acinetobacter baumannii*: emergence of a successful pathogen. Clin Microbiol Rev 2008;21:538–82.
[10] Hancock REW, Chapple DS. Peptide antibiotics. Antimicrob Agents Chemother 1999;43:1317–23.
[11] Beveridge TJ. Structures of Gram-negative cell walls and their derived membrane vesicles. J Bacteriol 1999;181:4725–33.
[12] Raetz CR, Whitfield C. Lipopolysaccharide endotoxins. Annu Rev Biochem 2002;71:635–700.
[13] Lewis LA, Choudhury B, Balthazar JT, Martin LE, Ram S, Rice PA, et al. Phosphoethanolamine substitution of lipid A and resistance of *Neisseria gonorrhoeae* to cationic antimicrobial peptides and complement-mediated killing by normal human serum. Infect Immun 2009;77:1112–20.
[14] Moskowitz SM, Ernst RK, Miller SI. PmrAB, a two-component regulatory system of *Pseudomonas aeruginosa* that modulates resistance to cationic antimicrobial peptides and addition of aminoarabinose to lipid A. J Bacteriol 2004;186:575–9.
[15] Winfield MD, Latifi T, Groisman EA. Transcriptional regulation of the 4-amino-4-deoxy-L-arabinose biosynthetic genes in *Yersinia pestis*. J Biol Chem 2005;280:14765–72.
[16] McPhee JB, Lewenza S, Hancock RE. Cationic antimicrobial peptides activate a two-component regulatory system, PmrA–PmrB, that regulates resistance to polymyxin B and cationic antimicrobial peptides in *Pseudomonas aeruginosa*. Mol Microbiol 2003;50:205–17.
[17] Adams MD, Nickel GC, Bajaksouzian S, Lavender H, Murthy AR, Jacobs MR, et al. Resistance to colistin in *Acinetobacter baumannii* associated with mutations in the PmrAB two-component system. Antimicrob Agents Chemother 2009;53:3628–34.
[18] Adams MD, Goglin K, Molyneaux N, Hujer KM, Lavender H, Jamison JJ, et al. Comparative genome sequence analysis of multidrug-resistant *Acinetobacter baumannii*. J Bacteriol 2008;190:8053–64.
[19] Gunn JS. The *Salmonella* PmrAB regulon: lipopolysaccharide modifications, antimicrobial peptide resistance and more. Trends Microbiol 2008;16:284–90.
[20] Fernandez-Reyes M, Rodriguez-Falcon M, Chiva C, Pachon J, Andreu D, Rivas L. The cost of resistance to colistin in *Acinetobacter baumannii*: a proteomic perspective. Proteomics 2009;9:1632–45.
[21] Moffatt JH, Harper M, Harrison P, Hale JDF, Vinogradov E, Seemann T, et al. Colistin resistance in *Acinetobacter baumannii* is mediated by complete loss of lipopolysaccharide. Antimicrob Agents Chemother 2010;54:4971–7.
[22] Dufrene YF. Using nanotechniques to explore microbial surfaces. Nat Rev Microbiol 2004;2:451–60.
[23] Beveridge TJ, Breznak JA, Marzluf GA, Schmidt TM, Snyder LR. Methods for general and molecular microbiology. 3rd ed. Washington, DC: ASM Press; 2007.
[24] Poudyal A, Owen RJ, Bulitta JB, Forrest A, Tsuji BT, Turnidge JD, et al. High initial inocula and stationary growth phase substantially attenuate killing of *Klebsiella pneumoniae* and *Acinetobacter baumannii* by colistin. In: Abstracts of the 48th Interscience Conference on Antimicrobial Agents and Chemotherapy (ICAAC). Washington, DC: ASM Press; 2008. p. 28 [Abstract A-1673].
[25] Li J, Milne RW, Nation RL, Turnidge JD, Coulthard K. Stability of colistin and colistin methanesulfonate in aqueous media and plasma as determined by high-performance liquid chromatography. Antimicrob Agents Chemother 2003;47:1364–70.
[26] Soon RL, Nation RL, Cockram S, Moffatt JH, Harper M, Adler B, et al. Different surface charge of colistin-susceptible and -resistant *Acinetobacter baumannii* cells measured with zeta potential as a function of growth phase and colistin treatment. J Antimicrob Chemother 2011;66:126–33.
[27] Doktycz MJ, Sullivan CJ, Hoyt PR, Pelletier DA, Wu S, Allison DP. AFM imaging of bacteria in liquid media immobilized on gelatin coated mica surfaces. Ultramicroscopy 2003;97:209–16.
[28] Soon RL, Nation RL, Hartley PG, Larson I, Li J. Atomic force microscopy investigation of the morphology and topography of colistin-heteroresistant *Acinetobacter baumannii* strains as a function of growth phase and in response to colistin treatment. Antimicrob Agents Chemother 2009;53:4979–86.
[29] Hutter JL, Bechhoefer J. Calibration of atomic force microscope tips. Rev Sci Instrum 1992;64:1868–73.
[30] Mendez-Vilas A, Gonzalez-Martin ML, Nuevo MJ. Some geometrical considerations about the influence of topography on the adhesion force as measured by AFM on curved surfaces. Appl Surf Sci 2004;238:9–13.
[31] Ducker WA, Senden TJ, Pashley RM. Direct measurement of colloidal forces using an atomic force microscope. Nature 1991;353:239–41.
[32] Ducker WA, Senden TJ, Pashley RM. Measurement of forces in liquids using a force microscope. Langmuir 1992;8:1831–6.
[33] Arnoldi M, Fritz M, Bauerlein E, Radmacher M, Sackmann E, Boulbitch A. Bacterial turgor pressure can be measured by atomic force microscopy. Phys Rev E Stat Phys Plasmas Fluids Relat Interdiscip Topics 2000;62:1034–44.
[34] Yongsunthon R, Lower SK. Force measurements between a bacterium and another surface in situ. Adv Appl Microbiol 2006;58:97–124.
[35] Scheuring S, Dufrene YF. Atomic force microscopy: probing the spatial organization, interactions and elasticity of microbial cell envelopes at molecular resolution. Mol Microbiol 2010;75:1327–36.
[36] Dufrene YF. Towards nanomicrobiology using atomic force microscopy. Nat Rev Microbiol 2008;6:674–80.
[37] Weisenhorn AL, Hansma PK, Albrecht TR, Quate CF. Forces in atomic force microscopy in air and water. Appl Phys Lett 1989;54:2651–3.
[38] Jonson AB, Normark S, Rhen M. Fimbriae, pili, flagella and bacterial virulence. Contrib Microbiol 2005;12:67–89.
[39] Lau PCY, Lindhout T, Beveridge TJ, Dutcher JR, Lam JS. Differential lipopolysaccharide core capping leads to quantitative and correlated modifications of mechanical and structural properties in *Pseudomonas aeruginosa* biofilms. J Bacteriol 2009;191:6618–31.
[40] Yao X, Walter J, Burke S, Stewart S, Jericho MH, Pink D, et al. Atomic force microscopy and theoretical considerations of surface properties and turgor pressures of bacteria. Colloids Surf B Biointerfaces 2002;23:213–30.
[41] Hancock RE. The bacterial outer membrane as a drug barrier. Trends Microbiol 1997;5:37–42.
[42] Li J, Nation RL, Owen RJ, Wong S, Spelman D, Franklin C. Antibiograms of multidrug-resistant clinical *Acinetobacter baumannii*: promising therapeutic options for treatment of infection with colistin-resistant strains. Clin Infect Dis 2007;45:594–8.
[43] Eaton P, Fernandes JC, Pereira E, Pintado ME, Xavier Malcata F. Atomic force microscopy study of the antibacterial effects of chitosans on *Escherichia coli* and *Staphylococcus aureus*. Ultramicroscopy 2008;108:1128–34.
[44] da Silva Jr A, Teschke O. Effects of the antimicrobial peptide PGLa on live *Escherichia coli*. Biochim Biophys Acta 2003;1643:95–103.
[45] Chen YY, Wu CC, Hsu JL, Peng HL, Chang HY, Yew TR. Surface rigidity change of *Escherichia coli* after filamentous bacteriophage infection. Langmuir 2009;25:4607–14.
[46] Mortensen NP, Fowlkes JD, Sullivan CJ, Allison DP, Larsen NB, Molin S, et al. Effects of colistin on surface ultrastructure and nanomechanics of *Pseudomonas aeruginosa* cells. Langmuir 2009;25:3728–33.
[47] Rivera M, Hancock RE, Sawyer JG, Haug A, McGroarty EJ. Enhanced binding of polycationic antibiotics to lipopolysaccharide from an aminoglycoside-supersusceptible, *tolA* mutant strain of *Pseudomonas aeruginosa*. Antimicrob Agents Chemother 1988;32:649–55.
[48] Peterson AA, Hancock RE, McGroarty EJ. Binding of polycationic antibiotics and polyamines to lipopolysaccharides of *Pseudomonas aeruginosa*. J Bacteriol 1985;164:1256–61.

Please cite this article in press as: Soon RL, et al. Effect of colistin exposure and growth phase on the surface properties of live *Acinetobacter baumannii* cells examined by atomic force microscopy. Int J Antimicrob Agents (2011), doi:10.1016/j.ijantimicag.2011.07.014

[49] Strauss J, Burnham NA, Camesano TA. Atomic force microscopy study of the role of LPS O-antigen on adhesion of *E. coli*. J Mol Recognit 2009;22: 347–55.
[50] Burks GA, Velegol SB, Paramonova E, Lindenmuth BE, Feick JD, Logan BE. Macroscopic and nanoscale measurements of the adhesion of bacteria with varying outer layer surface composition. Langmuir 2003;19: 2366–71.
[51] Amro N, Kotra L, Wadu-Mesthrige K, Bulychev A, Mobashery S, Liu G. High-resolution atomic force microscopy studies of the *Escherichia coli* outer membrane: structural basis for permeability. Langmuir 2000;16:2789–96.
[52] Lindhout T, Lau PC, Brewer D, Lam JS. Truncation in the core oligosaccharide of lipopolysaccharide affects flagella-mediated motility in *Pseudomonas aeruginosa* PAO1 via modulation of cell surface attachment. Microbiology 2009;155:3449–60.

Please cite this article in press as: Soon RL, et al. Effect of colistin exposure and growth phase on the surface properties of live *Acinetobacter baumannii* cells examined by atomic force microscopy. Int J Antimicrob Agents (2011), doi:10.1016/j.ijantimicag.2011.07.014